AD-A163 550 THEORY OF OCEAN-ARRAY INTERACTION PHASE I REPORT(U) 1/1
NAVAL UNDERWATER SYSTEMS CENTER NEW LONDON CT NEW
LONDON LAB R M KENNEDY ET AL 21 OCT 83 NUSC-TR-6863
UNCLASSIFIED F/G 8/3 NL

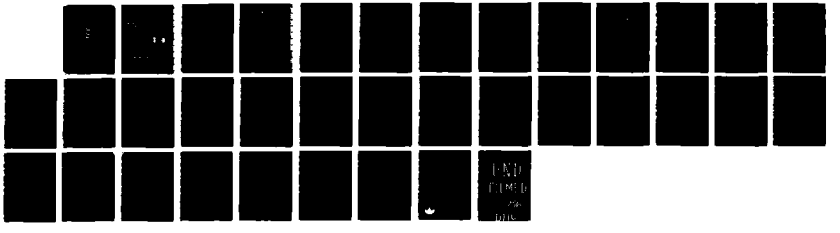

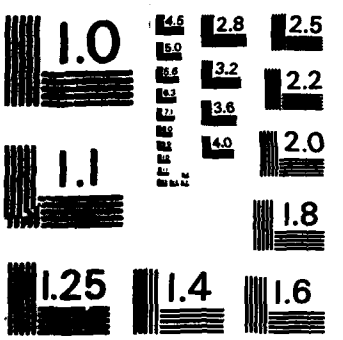

MICROCOPY RESOLUTION TEST CHART
NATIONAL BUREAU OF STANDARDS - 1963 - A

NUSC Technical Report 6863
21 October 1983

Theory of Ocean-Array Interaction, Phase I Report

Robert M. Kennedy
Submarine Sonar Department
Fort Lauderdale Detachment

Ding Lee
Submarine Sonar Department
New London Laboratory

Naval Underwater Systems Center
Newport, Rhode Island / New London, Connecticut

Preface

This report was prepared under Project No. A68055, Principal Investigator, R. Kennedy, and Program Manager, Dr. W. A. Vonwinkle. The work reported herein was performed as part of the Naval Underwater Systems Center program of Independent Research and Independent Exploratory Development (IR/IED).

Acknowledgment

The authors are grateful to Professor Murray Wachman, University of Connecticut, for his technical review of this document and his numerous helpful additions to the text.

The NUSC Technical Reviewer for this report was James M. Syck, Code 3341.

Reviewed and Approved: 21 October 1983

W. A. Von Winkle
Associate Technical Director for Technology

The authors of this report are located at the
Naval Underwater Systems Center,
Central Test and Evaluation Activity,
Fort Lauderdale, Florida 33315
and the
Naval Underwater Systems Center,
New London Laboratory,
New London, Connecticut 06320.

REPORT DOCUMENTATION PAGE		READ INSTRUCTIONS BEFORE COMPLETING FORM
1. REPORT NUMBER TR 6863	2. GOVT ACCESSION NO. AD-A163550	3. RECIPIENT'S CATALOG NUMBER
4. TITLE (and Subtitle) THEORY OF OCEAN-ARRAY INTERACTION, PHASE I REPORT		5. TYPE OF REPORT & PERIOD COVERED 6. PERFORMING ORG. REPORT NUMBER
7. AUTHOR(s) Robert M. Kennedy Ding Lee		8. CONTRACT OR GRANT NUMBER(s)
9. PERFORMING ORGANIZATION NAME AND ADDRESS Naval Underwater Systems Center New London Laboratory New London, CT 06320		10. PROGRAM ELEMENT, PROJECT, TASK AREA & WORK UNIT NUMBERS
11. CONTROLLING OFFICE NAME AND ADDRESS		12. REPORT DATE 21 October 1983 13. NUMBER OF PAGES
14. MONITORING AGENCY NAME & ADDRESS(if different from Controlling Office)		15. SECURITY CLASS. (of this report) UNCLASSIFIED 15a. DECLASSIFICATION/DOWNGRADING SCHEDULE

16. DISTRIBUTION STATEMENT (of this Report)

17. DISTRIBUTION STATEMENT (of the abstract entered in Block 20, if different from Report)

Approved for public release; distribution unlimited.

18. SUPPLEMENTARY NOTES

19. KEY WORDS (Continue on reverse side if necessary and identify by block number)

Towed array
Hydrodynamics

20. ABSTRACT (Continue on reverse side if necessary and identify by block number)

This report discusses a linear model that describes the transverse dynamics of a cable/towed array system driven by oceanic crosscurrents. This model was derived during the first phase of an Ocean-Array Interaction study. Solutions of the governing momentum equation show the characteristics of transverse dynamics of the system. The cable/towed array system attempts to align locally with the fluid flow axis but is impeded by the tension stiffness of the system. The result is that the transverse displacement response of the system is proportional to the local fluid

DD FORM 1 JAN 73 1473 EDITION OF 1 NOV 65 IS OBSOLETE
S/N 0102-014-6601

20. (Cont'd)

angle (V/U) and the ratio of normal to transverse hydrodynamic drag (c_n/c_t), and is inversely proportional to a power of the oceanic alongtrack wavenumber (k^n), where n = 0 for small wavenumbers and n = 2 for large wavenumbers. Diminishing longitudinal tension near the free end creates the appearance of a "tail wagging" which is more pronounced at high wavenumbers. The actual response to oceanic forcing is determined by the Fourier Bessel spectra of a function of the spatial distribution of crosstrack ocean current structure that determines which "modes" of behavior are excited. A numerically efficient solution to the governing equation using the "method of lines" and "generalized Adams-Bashforth methods" was developed and examples were run.

Keywords:

Towed arrays; Hydrodynamics.

Table of Contents

List of Illustrations

THEORY OF OCEAN-ARRAY INTERACTION, PHASE I REPORT

1. INTRODUCTION

A linear model describing the transverse dynamics of a long flexible cylinder in axial flow is presented in references 1 and 2. Experimental verification of the theory is discussed in reference 3. That work describes the transverse response of the cylinder to a forced vibration at the upstream end of the cylinder.

The analytical procedure of the previous work involved solving a homogeneous momentum equation in which the forced vibration entered through the upstream boundary condition. The solution modeled a cable/towed array system excited by the random crosstrack meandering of the towing vessel. In this study we are concerned with the transverse dynamics of a long flexible cylinder in "nearly" axial flow. In the present case, a space-time field of fluid flow orthogonal to the axial flow is superimposed on the basic axial flow. This crosscurrent is a perturbing flow that always has a magnitude much smaller than the axial flow. The intent of this study was to model the transverse dynamics of a cable/array system driven by crosscurrents.

Analytically, the procedure in the present work involved solving the same previously discussed momentum equation, only now modified to be nonhomogeneous with the oceanic excitation entering through the nonhomogeneous term.

The nonhomogeneous governing equation is derived and discussed in section 2. Approximate solutions relevant to low- and high-frequency domains of interest are discussed in section 3. In section 4, a complete solution is developed and a numerical technique is applied to the problem in section 5. The work is summarized in section 6. Excitation of the system by a plane wave is discussed in each section.

2. GOVERNING EQUATION

2.1 MOMENTUM EQUATION

The basic partial differential equation (PDE) applied in this study was derived and discussed in several papers.[1,4,5] The equation describes the dynamics of a physical configuration (see figure 1). The configuration consists of a flexible cylindrical body of circular cross-section that is immersed in an incompressible

fluid of uniform density. The fluid is flowing* with uniform velocity (U) parallel to the x axis.[2] The equation is expressed as

$$(M + m)\frac{\partial^2 y}{\partial t^2} + MU^2\frac{\partial^2 y}{\partial x^2} + 2MU\frac{\partial^2 y}{\partial x \partial t} - \frac{\partial}{\partial x}\left[2c_t \frac{M}{d_c} U^2 (L - x)\frac{\partial y}{\partial x}\right] + \frac{2c_n}{\pi}\frac{MU}{d_c}\left(\frac{\partial y}{\partial t} + U\frac{\partial y}{\partial x}\right) = 0 , \quad (1)$$

where

- $y(x,t)$ = crosstrack position of the cylinder measured at x,
- x = alongtrack independent space variable increasing downstream,
- t = time,
- M = effective mass of fluid "pushed" by the cylinder per unit length of cylinder,
- m = mass of the cylinder per unit length,
- U = free stream velocity,
- L = cylinder length,
- d_c = cylinder diameter,
- c_t = tangential (longitudinal) drag coefficient, and
- c_n = coefficient of the linearized normal drag expression.

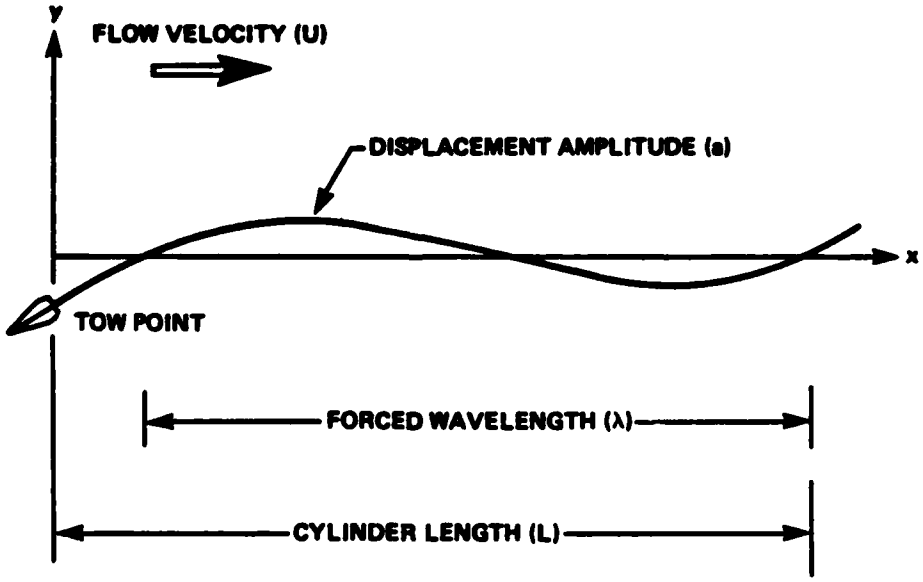

Figure 1. Towing System Coordinates

*Or, equivalently, being towed with uniform velocity (U).

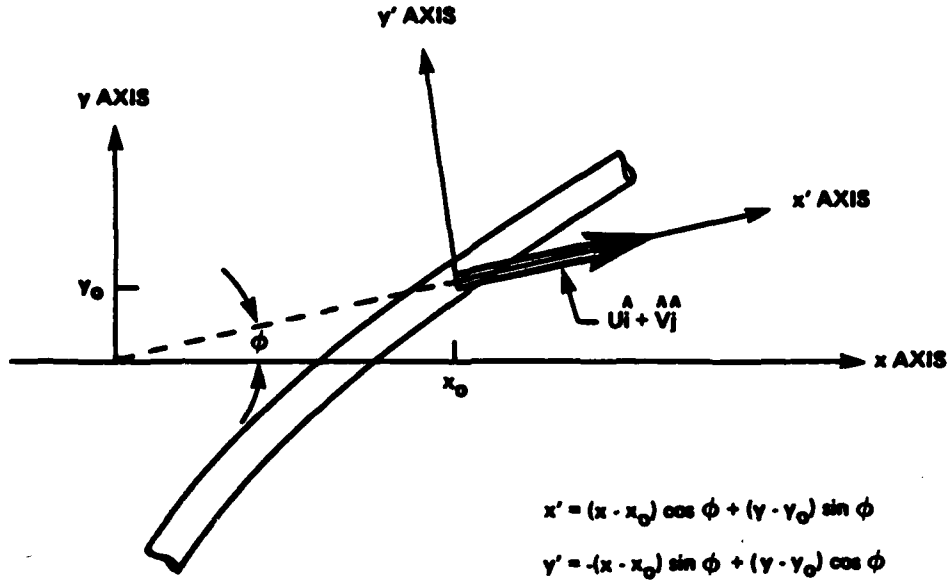

Figure 2. Modified Coordinate System

The effect of a current component, $\hat{V}$, in the y direction is to modify the original flow from $U\hat{i}$ to $U\hat{i} + \hat{V}\hat{j}$, where $\hat{i}$ and $\hat{j}$ are unit vectors in the coordinate system of figure 1. This flow modification is important when examining the hydrodynamic terms. It is important to recognize that because hydrodynamic forces are nonlinearly related to fluid velocities, we cannot calculate the Cartesian components of the force directly from the Cartesian coordinates of the fluid velocity. We must first find the total fluid velocity and direction and then the resultant vector force. Figure 2 shows the geometric relationships. Note that the figure ignores the small angle assumptions inherent in the derivation of equation (1) in order to improve the geometric visualization.

The cylinder is towed in the negative x direction creating, in the translating coordinate systems of figures 1 and 2, a flow component, U, in the positive x direction. The crossflow, V, is in the positive y direction which creates a local total fluid velocity having polar coordinates $U\,[1 + (\hat{V}/U)^2]^{1/2}$ and ϕ. This is a space-time function because

$$\hat{V} = \hat{V}(x,t) \ .$$

The normal hydrodynamic drag on the cylinder is well known to be

$$\frac{1}{2}\rho d_c U^2 \left[1 + \left(\frac{\hat{V}}{U}\right)^2\right] f(\alpha) \ ,$$

where α is the angle between the fluid velocity vector and the tangent to the cylinder at a point. The form of $f(\alpha)$ used in reference 1 and later experimentally supported in reference 6 may be written as

$$f(\alpha) = \begin{cases} c_n \sin \alpha \text{ for } \alpha \leq 3^\circ \\ c_n' \sin^2 \alpha \text{ for } \alpha > 3^\circ \end{cases} .$$

Typical numerical values of these coefficients[1,6] are $c_n = 1.2$ and $c_n' = 0.07$. A basic assumption of equation (1) is that $\alpha < 3°$. Here we are further going to require that

$$\hat{V}/U << 1 .$$

Thus, the normal hydrodynamic drag becomes

$$1/2\rho d_c c_n U^2 \alpha \quad \text{for } \alpha < 3^\circ . \tag{2}$$

Lighthill[7] showed that the fluid velocity relative to the cylinder and normal to the axis of the cylinder is

$$\frac{\partial y'}{\partial t} + U \frac{\partial y'}{\partial x'} ,$$

where y' and x' are coordinates determined by the total fluid flow, $U\hat{i} + \hat{V}\hat{j}$, and are defined in figure 2. We again assumed that $\hat{V}/U << 1$. Following Paidoussis,[4] we make the small angle approximation*

$$\alpha \simeq \frac{\frac{\partial y'}{\partial t} + U \frac{\partial y'}{\partial x'}}{U} , \tag{3}$$

and introduce the variable

$$\phi = \hat{V}/U .$$

The transformation from the primed to unprimed coordinate system is shown in figure 2. x_o, y_o is an arbitrary position and can be taken to be zero. Following the rules of partial derivatives we may write the following relations:

$$\frac{\partial y'}{\partial x'} = -(x + y \tan \phi) \frac{\partial \phi}{\partial x} - \sin \phi + \frac{\partial y}{\partial x}$$

and

$$\frac{\partial y'}{\partial t} = -(x + y \sin \phi) \frac{\partial \phi}{\partial t} - \sin \phi \frac{\partial x}{\partial t} + \cos \phi \frac{\partial y}{\partial t} .$$

*Note that α is expressible as the arcsine of the normal and axial components of flow velocity.

The small angle assumption allows the following relations: $\cos \cong 1$ and $\sin \phi \cong \phi \cong \tan \phi$ and $\partial x/\partial t \cong 0$. Thus the partial derivatives become

$$\frac{\partial y'}{\partial x'} = \frac{\partial y}{\partial x} - \phi + \left[(x + y\phi) \frac{\partial \phi}{\partial x} \right] \tag{4a}$$

and

$$\frac{\partial y'}{\partial t} = \frac{\partial y}{\partial t} - \left[(x + \phi y) \frac{\partial \phi}{\partial t} \right] . \tag{4b}$$

Because the transformations are "local" (i.e., they are applied at $x = y = 0$), we may substitute the expressions

$$\frac{\partial y'}{\partial x'} = \frac{\partial y}{\partial x} - \frac{\hat{V}}{U}$$

and

$$\frac{\partial y'}{\partial t} = \frac{\partial y}{\partial t}$$

into equation (3). This makes the normal hydrodynamic term equal to

$$\frac{1}{2}\rho d_c C_n U \left(\frac{\partial y}{\partial t} + U \frac{\partial y}{\partial x} \right) - \frac{1}{2}\rho d_c U \hat{V} .$$

We may modify this equation by eliminating[4,5] ρ using the form

$$\rho = 4M/\pi d_c^2 ,$$

yielding

$$\frac{2c_n}{\pi} \frac{MU}{d_c} \left(\frac{\partial y}{\partial t} + U \frac{\partial y}{\partial x} \right) - \frac{2c_n}{\pi} \frac{MU}{d_c} \hat{V} . \tag{5}$$

The first term above already appears in equation (1). The second term is the nonhomogeneous addition and becomes the right-hand side of our present problem.

Note that the presence of $\hat{V}$ in the problem does not alter the inertial terms of equation (1) and, assuming $\hat{V}/U \ll 1$, does not alter the tension term either.

The following nondimensional variables are introduced into equation (1) modified by equation (5):

$$\tau = \frac{tU}{L} , \quad \xi = \frac{x}{L} , \quad \eta = \frac{y}{\Delta} , \quad \beta = \frac{M}{M + m} , \quad \varepsilon = \frac{L}{d_c} , \text{ and } V = \frac{\hat{V}}{U} , \tag{6}$$

where Δ is an arbitrary length which can take on any value because equation (1) is linear in y. The result is

$$\frac{\partial^2\eta}{\partial\tau^2} + 2\beta\frac{\partial^2\eta}{\partial\tau\partial\xi} + (a + b\xi)\frac{\partial^2\eta}{\partial\xi^2} + c\frac{\partial\eta}{\partial\xi} + d\frac{\partial\eta}{\partial\tau} = -dV \text{ for } 0 \leq \xi \leq 1 \ , \quad (7)$$

where

$$a = \beta(1 - 2c_t\varepsilon) \ ,$$

$$b = 2\beta c_t\varepsilon \ ,$$

$$c = 2(c_t + c_n/\pi)\varepsilon\beta \ , \text{ and}$$

$$d = (2/\pi)\beta c_n\varepsilon \ .$$

The dependence of the nonhomogeneous term of equation (7) on c_n is intuitively clear, however, the dependence on ε is not as obvious. The role of ε in that term is to show the relative importance of the nonhomogeneous hydrodynamic forcing function relative to the inertial forces, i.e., the first two terms of equation (7). Large values of ε reduce the inertial effects. β for a cylinder at relatively small frequencies is a constant (i.e., 1/2).

2.2 BOUNDARY CONDITIONS

The appropriate boundary conditions have been discussed in references 1, 4, 5, and 8. Two boundary conditions are required for the second-order description of equation (7). In general, the upstream ($\xi = 0$) boundary condition is an arbitrary time function, that is,

$$\eta(\xi = 0, \tau) = g(\tau) \ .$$

For a boundary condition on the downstream end of the cable ($\xi = 1$), we encounter a fundamental problem that is a consequence of dropping the flexural rigidity term in the Paidoussis momentum equation. Because the physical constraint at the free end involves bending moments, the second-order system (which allows no bending moments) is unable to characterize the free end physical condition. Analytically, this problem results from changing from a fourth-order to a second-order description.

Historically, this type of problem (D. Bernoulli's "hanging chain," 1732) has been solved by invoking a boundedness condition, that is,

$$|\eta(\xi,\tau)| < \infty \quad \text{for} \quad 0 \leq \xi \leq 1 \ .$$

It will be useful to think of the nondimensional displacement, η, as consisting of two additive terms, that is,

$$\eta = \eta_1 + \eta_2 \ .$$

Thus, with the linear operator D defined by equation (7) we may write

$$D\eta(\xi,\tau) = -dV(\xi,\tau) \qquad \text{for } 0 \leq \xi \leq 1 \ , \qquad (7a)$$

with

$$\eta(\xi,\tau) = g(\tau) \qquad \text{for } \xi = 0$$

and

$$|\eta(\xi,\tau)| < \infty \qquad \text{for } 0 \le \xi \le 1 ,$$

or, equivalently, we have the system of equations

$$\begin{aligned} D\eta_1(\xi,\tau) &= 0 && \text{for } 0 \le \xi \le 1 . \\ \eta_1(\xi,\tau) &= g(\tau) && \text{for } \xi = 0 . \\ |\eta_1(\xi,\tau)| &< \infty && \text{for } 0 \le \xi \le 1 . \end{aligned} \tag{7b}$$

and

$$\begin{aligned} D\eta_2(\xi,\tau) &= -dV(\xi,\tau) && \text{for } 0 \le \xi \le 1 . \\ \eta_2(\xi,\tau) &= 0 && \text{for } \xi = 0 . \\ |\eta_2(\xi,\tau)| &< \infty && \text{for } 0 \le \xi \le 1 . \end{aligned} \tag{7c}$$

Thus η_1 and η_2 are solutions to two types of problems: (1) η_1 is the solution to the homogeneous momentum equation and is the response to the forced vibration problem discussed in references 1 and 2, and (2) η_2 is the solution to the nonhomogeneous equation and is the response to the crossflow. Note that in general η_2 will equal the sum of "modes" which have zero displacement at the upstream end.

2.3 NONHOMOGENEOUS TERM

In a very general sense the ocean space-time field may be thought of as an addition of plane waves and may be written as

$$\hat{V} = \sum_{\vec{k}} A_{\vec{k}}(t) e^{i(\omega_k t - \vec{k}\cdot\vec{x})} . \tag{8}$$

where $\vec{k}$ is a two-dimensional wavenumber and the summation is overall values of $\vec{k}$.

Because we are primarily concerned with towed sensors, we must account for Doppler effects. If we are towing in a direction parallel to the negative x direction at the speed U, and we are located along the cylinder at the position x, the argument of the exponent of equation (8) becomes

$$k \sin \phi_k U t - k \sin \phi_k x + \omega_k t , \tag{9}$$

where $|\vec{k}| = |\vec{k}|$ and ϕ_k is the angle of k with respect to the y axis. The oceanic process will have a phase velocity, C_k, defined from the dispersion relation, $kC_k = \omega_k$. Equation (8) thus becomes

$$\hat{V}(x,t) = \sum_{\vec{k}} A_{\vec{k}}(t) e^{i[(\omega_k + k_x U)t - k_x x]} , \tag{10}$$

where $\omega_k + k_x U$ is a Doppler-shifted angular frequency and k_x is the x component of $\vec{k}$. Thus, in the translating array coordinate system the ocean currents appear like plane waves traveling in the positive x direction and having an alongtrack wave number, k_x, and a frequency, $k_x (C_k + U)$. Typically, $C_k \ll U$. These can be superimposed in the usual Fourier sense.

We next drop the x subscript on the wavenumber and recognize that the wavenumber, k, is the alongtrack wavenumber. The argument of the exponent in equation (10) may be written as

$$k\left[(C_k + U)t - x\right] = kL\left[\left(\frac{C_k}{U} + 1\right)\frac{Ut}{L} - \frac{x}{L}\right]$$

which is

$$\hat{k}[(\hat{C}_k + 1)\ T - \xi] \ ,$$

where the "hat" denotes a nondimensional variable. Henceforth, in this report the "hat" will be dropped and k, C_k, and ω will be nondimensional.

3. APPROXIMATE SOLUTIONS

Approximate solutions that apply to low- and high-frequency regions are explored in this section because they lead to a physical understanding of the process.

3.1 LOW-FREQUENCY APPROXIMATION

Using a perturbation technique to solve equation (1), it was shown[2] that an important solution to the forced vibration problem occurs when the forced vibration frequency is small,[3] that is, when $\omega L/U < 1$. A low-frequency vibration convects back along the cylinder relatively unattenuated. At higher frequencies significant viscous damping and structural stiffness take place. Thus, in actual towed systems typically subjected to a range of excitation frequencies, the principal dynamics take place at the lowest frequencies. A similar result would be anticipated in our present non-homogeneous case, i.e., equation (7).

Reference 2 shows that in the low-frequency approximation the inertial force,

$$\frac{\partial^2 \eta}{\partial \tau^2} + 2\beta \frac{\partial^2 \eta}{\partial \xi \partial \tau} \ ,$$

and the second-order part of the tension stiffness, $(a + b)\ \partial^2\eta/\partial\xi^2$, are negligible relative to the hydrodynamic forces and the first-order part of the tension stiffness, i.e.,

$$c\frac{\partial \eta}{\partial \xi} \ .$$

Note that the two parts of the tension force are a consequence of the linearly decreasing tension of a towed sensor. We see that in dimensional quantities

$$\frac{\partial}{\partial x}\left(T(x)\,\frac{\partial y}{\partial x}\right) = T(x)\,\frac{\partial^2 y}{\partial x^2} + \frac{\partial T(x)}{\partial x}\,\frac{\partial y}{\partial x}\quad , \tag{11}$$

where $\partial T(x)/\partial x$ is a constant and T is tension. Thus, the low-frequency approximation to equation (7) is

$$\frac{\partial \eta}{\partial \tau} + c_o\,\frac{\partial \eta}{\partial \xi} = V\ , \tag{12}$$

where

$$c_o = 1 + \frac{\pi c_t}{c_n}\quad .$$

References 6 and 9 show experimentally that $\pi c_t/c_n$ is of order 10^{-1}.

Following reference 7, we let $u(\xi,\tau,\eta)$ = constant be an integral of equation (12). Then

$$\frac{\partial u}{\partial \xi} + \frac{\partial u}{\partial \eta}\,\frac{\partial \eta}{\partial \xi} = 0 \qquad \text{and} \qquad \frac{\partial u}{\partial \tau} + \frac{\partial u}{\partial \eta}\,\frac{\partial \eta}{\partial \tau} = 0 \tag{13}$$

Substitution of equation (13) into (12) yields

$$\frac{\partial u}{\partial \tau} + c_o\frac{\partial u}{\partial \xi} + V\frac{\partial u}{\partial \eta} = 0\ , \tag{14}$$

which may be written as a vector product

$$(\hat{i} + c_o\hat{j} + V\hat{k}) \cdot \nabla u = 0\ , \tag{15}$$

where $\hat{i}$, $\hat{j}$, and $\hat{k}$ are unit base vectors in a Cartesian coordinate system and Δ is the gradient operator. Thus the vector $\hat{i} + c_o\hat{j} - Vk$ is perpendicular to the normal to u and is thus tangent to a solution surface.

The vector indicates the direction in ξ,τ,η space taken by the solution. The path taken by a "particle" in the solution space is called the characteristic of the equation. The equation for the characteristic is

$$d\tau = \frac{d\xi}{c_o} = \frac{d\eta}{V}\quad , \tag{16}$$

which defines two ordinary differential equations that have the integrals

$$u_1(\xi,\tau,\eta) = C_1 \qquad \text{and} \qquad u_2(\xi,\tau,\eta) = C_2\ .$$

Any intersection of these two surfaces is the characteristic curve. The intersection occurs[10] whenever

$$u_1 = f(u_2)\ ,$$

where f( ) is an arbitrary function. The integrals of $c_o d\tau = d\xi$ and $-Vd\xi = c_o d\eta$ are

$$u_1 = \xi - c_o\tau = c_1 \tag{18a}$$

and

$$u_2 = \eta + \frac{1}{c_o} \int d\xi V = c_2 \ . \tag{18b}$$

The intersection of u_1 and u_2 surfaces gives the solution

$$\eta - \frac{1}{c_o} \int d\xi V = f(\xi - c_o \tau) \ , \tag{19}$$

where f( ) may be evaluated from the upstream boundary condition, $\eta(0,\tau) = g(\tau)$.

In the previous section we saw that V may be written as the sum of plane waves. Thus we are interested in the integral

$$\int d\xi V = \frac{|V|}{ik} e^{ik[(c_k + 1)\tau - \xi]} + K(\tau) \text{ for } k < 1 \ , \tag{20}$$

where $k(\tau)$ is the integration constant. The solution we seek then becomes

$$\eta(\xi,\tau) = f(\xi - c_o\tau) + \xi\phi \frac{e^{ik[(c_k + 1)\tau - \xi]}}{ik\xi} - K(\tau) \ ,$$

where $\phi = |v|/c_o$.

In order to meet the upstream boundary condition, that is,

$$\eta(0,\tau) = g(\tau) \ ,$$

we set

$$f( ) = g( )$$

and

$$K(\tau) = - \frac{e^{+ik(c_k + 1)\tau}}{ik} \phi \ .$$

With these conditions the solution becomes

$$\eta(\xi,\tau) = g(\xi - c_o\tau) + \xi\phi \frac{e^{i[k(c_k + 1)\tau - k\xi]}}{ik\xi} (e^{ik\xi} - 1)$$

for $k<1$. For $k<1$ it is useful to make the approximation

$$\frac{e^{ik\xi} - 1}{ik\xi} \simeq \frac{1}{ik\xi} \left(-ik\xi - \frac{k^2\xi^2}{2} + \ldots \right) \ .$$

Thus to first order, the solution is

$$\eta(\xi,\tau) = g(\xi - c_o\tau) + \xi\phi e^{i[(\omega_k + \omega)\tau - k\xi]} \text{ for } k < 1 \ . \tag{21}$$

The solution contains two parts: (1) the boundary condition propagating downstream nondispersively with the velocity c_o, and (2) the nonhomogeneous forcing functions resulting in an additive solution that is proportional to the magnitude of the angle of the local fluid velocity, $|v|/c_o$. Physically, this is a consequence of the cylinder's natural tendency to align itself with the flow, which in this case is the orthogonal addition of U and $\hat{V}$. Actually the magnitude of the cylinder slope with respect to the x axis is not proportional to $\hat{V}/U$ as might be thought, but rather is

$$\frac{\hat{V}}{Uc_o} \sin \hat{k}\,[(c_k + 1)Ut - x] \quad . \tag{22}$$

Physically, the actual angle is decreased by the impedance of the slope-dependent tension stiffness (equation (11)) term, c_o. Because the cylinder nearly aligns with the flow, the displacements are the spatial integral of the slope, which enters the wavenumber in the denominator.

The $f(\xi - c_o\tau)$ term in equations (19) and (21) is the "water pulley" effect described by Kennedy.[2]

Noting from equations (16) and (22) that the space-time slope of the cylinder is $-V/c_o$ we may rewrite equation (19) as

$$\eta(\xi,\tau) = g(\xi - c_o\tau) - \int d\xi\theta(\xi,\tau) \quad , \tag{23}$$

where we use a small angle approximation for θ which is explicit in the derivation of equation (1). Thus we see that at low frequencies the particular integral of equation (7) results from the cylinder locally aligning with the flow so as to minimize the hydrodynamic resistance. The shape of the system is then the spatial integral of the slope by definition.

3.2 HIGH-FREQUENCY APPROXIMATION

Returning to the PDE of equation (7), we again summarize the coefficients as

$$\begin{aligned} a &= \beta - 2\beta c_t \varepsilon \quad , \\ b &= 2\beta c_t \varepsilon \quad , \\ c &= 2\varepsilon\beta\,(c_t + c_n/\pi) \quad , \text{ and} \\ d &= 2\beta\varepsilon\frac{c_n}{\pi} \quad . \end{aligned} \tag{24}$$

A significant simplification results from exploiting the fact that the cylinders of interest have quite high aspect ratios, that is, ε is large. A further simplification results from neglecting $c_t\pi/c_n$ relative to unity. As noted previously, $c_t\pi/c_n$ is of order 10^{-1}. Thus, if $\varepsilon \to \infty$ equation (7) becomes

$$(1 - \xi)\frac{\partial^2\eta}{\partial\xi^2} - \frac{c_n}{\pi c_t}\frac{\partial\eta}{\partial\xi} - \frac{c_n}{\pi c_t}\frac{\partial\eta}{\partial\tau} = \frac{c_n}{\pi c_t} V \quad . \tag{25}$$

From the discussion following equation (10) we see that high frequencies are equivalently high wavenumbers because $\omega \cong kU$. Thus, a high-frequency approximation is equivalently a high wavenumber approximation. Again following the procedures of reference 2, we make a WKB-like approximation in assuming that $\partial^2\eta/\partial\xi^2$ changes rapidly during small changes in $(1 - \xi)$. If, therefore, $(1 - \xi)$ is treated as a constant, then equation (25) becomes a linear PDE with constant coefficients.* Because, in this approximation, the cylinder takes on numerous cycles and our motivation is only to identify physical mechanisms, we simplify the problem by neglecting the boundary conditions and making the cylinder infinitely long. If we let

$$\eta(\xi,\tau) = r(\tau)e^{-ik\xi} , \tag{26}$$

then equation (25) becomes

$$\left[-k^2(1 - \xi) + ik \frac{c_n}{\pi c_t} c_o\right] r(\tau) - \frac{c_n}{\pi c_t} \frac{dr(\tau)}{d\tau} = \frac{c_n}{\pi c_t} V(\xi,\tau)e^{ik\xi} . \tag{27}$$

The Laplace transform of equation (27) for the case of zero initial conditions is

$$R(s)\ (s + Q) = -V(\xi,s)\ e^{ik\xi} \tag{28}$$

where R and V are transforms of r and V, s is the transform variable, and

$$Q = -ikc_o + k^2 \frac{\pi c_t}{c_n} (1 - \xi) . \tag{29}$$

Directing our interest to the plane wave case, that is, $V(\xi,\tau) = V \exp i(\omega\tau - k\xi)$, we have

$$R(s) = \frac{-|V|}{(s + Q)(s - i\omega)} . \tag{30}$$

The inverse transform is

$$r(\tau) = -|V|\ A(e^{-Q\tau} - e^{i\omega\tau}) , \tag{31}$$

where

$$A = (Q - i\omega)^{-1}$$

or

$$A^{-1} = \frac{\pi c_t}{c_n} (1 - \xi)k^2 + i(kc_o - \omega)$$

$$= \frac{\pi c_t}{c_n} (1 - \xi)k^2 \left[1 + i \frac{(kc_o - \omega) \frac{c_n}{\pi c_t}}{(1 - \xi)k^2}\right] . \tag{32}$$

*It was found in reference 3 that this approximation leads to an adequate model for $k > 50$ and $\xi < 0.98$.

For our current large k case,

$$\frac{(kc_o - \omega)\,\frac{c_n}{\pi c_t}}{(1 - \xi)k^2} << 1 \quad . \tag{33}$$

Therefore,

$$A \simeq \frac{\frac{c_n}{\pi c_t}}{k^2(1 - \xi)} \left[1 - i\,\frac{\frac{c_n}{\pi c_t}(kc_o - \omega)}{(1 - \xi)k^2} + \ldots\right]$$

$$\simeq \frac{\frac{c_n}{\pi c_t}}{k^2(1 - \xi)}\, e^{i\psi} \quad , \tag{34}$$

where

$$\tan \psi = \frac{\frac{c_n}{\pi c_t}(kc_o - \omega)}{k^2(1 - \xi)} \quad . \tag{35}$$

Finally we write

$$\eta(\xi,\tau) = \frac{|V|\,\frac{c_n}{\pi c_t}}{k^2(1 - \xi)}\, e^{i\psi} \left\{ e^{i(\omega\tau - k\xi)} - e^{-k^2 \frac{\pi c_t}{c_n}(1 - \xi)\tau}\, e^{i(kc_o\tau - k\xi)} \right\} \tag{36}$$

for $k > 50$ and $\xi < 0.9$.

Because of the large values of k necessary for this approximation, to hold the second term in the brackets rapidly becomes negligible, and the solution is a wave propagating downstream at the tow speed.

The amplitude of the wave is exactly the ratio of the normal hydrodynamic force applied by the crosscurrent on the cylinder to the tension stiffness of the cylinder tensioned by tangential hydrodynamic drag for a sinusoidally perturbed cylinder. Using a hat to denote dimensional quantities we show the above statement by noting

that the normal force to the cylinder* is $1/2\varrho Dc_n U\hat{V}$, and the tension stiffness is $T(x)\partial^2 y/\partial x^2$ where $T(x) = 1/2\varrho Dc_t LU^2(1 - x/L)$. Thus, if the induced shape is assumed sinusoidal with maximum amplitude A and wavenumber $\hat{k}$, then the two forces will balance when

$$A = \frac{\left(\frac{\hat{V}}{U}\right)\left(\frac{c_n}{\pi c_t}\right)}{\hat{k}^2(1 - \xi)L} \tag{37}$$

which in nondimensional form is exactly the amplitude of equation (36). Thus the amplitude of the wave is determined by string-like forces, but not the propagation velocity. The significant amplitude attenuation caused by tension stiffness is reduced as $(1 - \xi)^{-1}$ reflecting the tension reduction as one approaches the free end.

4. COMPLETE SOLUTION

The discussion in this section is limited to the solution to equation (7c) because the solution to equation (7b) has been detailed in reference 1. The subscript (η_1) of equation (7c) will be dropped to increase notational efficiency.

In solving equation (7c), we make the fundamental assumption that the solution of $\eta(\xi,\tau)$ is separable in space and time, and the time dependence is harmonic, that is,

$$\eta(\xi,\tau) = S(\xi)e^{i\omega\tau}$$

$$\nu(\xi,\tau) = \nu'(\xi)^{i\omega\tau}$$

where ω is noted to be nondimensional and, in general, complex, and i denotes the imaginary number. Note that after the substitution the primes are dropped.

Substituting the above equation into equation (7c), along with the transformation of the independent spatial variable ($z^2 = a + b\xi$), yields the ordinary differential equation (ODE)

$$\frac{d^2S}{dz^2} + \frac{a_o}{z}\frac{dS}{dz} + b_o^2 S = c_o V \quad \text{for } 0 \le z^2 \le a \tag{38}$$

with the boundary conditions

$$S(z) = 0 \quad \text{for } z^2 = a\ ,$$

$$|S(z)| < \infty \quad \text{for } 0 \le z^2 \le a\ ,$$

*This form was originally used by Paidoussis in reference 4 and more recently by Ketchman in reference 11.

where

$$a_o = \frac{2}{b}(c + 2i\omega\beta) - 1 ,$$

$$b_o^2 = \frac{4\omega}{b^2}(id - \omega) , \text{ and}$$

$$c_o = \frac{4d}{b^2} .$$

Equation (38) is recognized as a modified form of Bessel's equation.[5]

It is useful to make the transformation

$$w(z) = S(z)z^p , \tag{39}$$

where

$$p = \frac{a_o - 1}{2} .$$

After some algebra the governing ODE becomes

$$\mathcal{L}w + \lambda^2 zw = c_o z^{p+1} V(z) , \tag{40}$$

where $\mathcal{L}$ is the Sturm-Liouville operator[10]

$$\mathcal{L} = \frac{d}{dz}\left(z \frac{d}{dz}\right) - \frac{p^2}{z}$$

containing the coefficients of Bessel's equation and λ^2 equals b_o^2 . The boundary conditions for this problem are

$$w(z) = 0 \quad \text{for } z = a^{1/2} , \tag{41}$$

and w(z) is finite.

Much has been written of the Sturm-Liouville problem. An important aspect of this classical ODE, pertaining to our present problem, is that because z vanishes at the upstream end of the interval (i.e., z = 0), and the solution vanishes at the other end of the interval (i.e., $w(a^{1/2}) = 0$), then the Eigenfunctions of

$$\mathcal{L}w_n + \lambda_n^2 z w_n = 0 \tag{42}$$

are orthogonal with respect to the weighting function z over the interval 0 to $a^{1/2}$, and λ_n^2 are Eigenvalues that satisfy the boundary conditions.
Thus,

$$\int_0^1 z w_n w_m dz = 0 \quad \text{if } n \neq m \quad . \tag{43}$$

Actually this differs somewhat from our problem in that the interval is $a^{1/2}(1 + b/a)$ to $a^{1/2}$, not 0 to $a^{1/2}$. This is a consequence of the switching of equation (1) from the hyperbolic PDE to an elliptic PDE quite near the downstream end.[1] All of the above mathematics apply only in the hyperbolic region. The switchover point[1] occurs when

$$\xi = a/b \quad . \tag{44}$$

Thus, if a/b is unity the switch does not take place until the end of the cylinder is encountered and the interval of z becomes 0 to 1. Writing

$$-a/b = 1 - 1/2c_t\varepsilon \tag{45}$$

we see that this condition is nearly approached for long cylinders. We assume that this condition is met.

Because equation (42) is the classical Bessel equation, the Eigenfunctions are Bessel functions of the first and second kind. Bessel functions of the second kind will be singular in the interval of interest, thus they are excluded by the finite condition[1] of equation (41). Therefore, the complete solution to equation (42) with the boundary conditions of equation (41) is

$$w(z) = \sum_n b_n J_p(\lambda_n z) \quad \text{for } 0 \leq z \leq a^{1/2} \quad , \tag{46}$$

where

$$p = \frac{c_n}{\pi c_t} + i \frac{\omega}{c_t \varepsilon} \tag{47}$$

and $\lambda_n a^{1/2}$ are the zeros of the Bessel function. Following reference 1 we avoid the complication of complex-order Bessel functions by again requiring a long cylinder, long enough so that

$$|\omega|/(c_t\varepsilon) << c_n/\pi c_t \quad .$$

With this condition met all λ_n are real numbers. The coefficients, b_n, are found from initial conditions.

Because of the orthogonality of the Eigenfunctions the nonhomogeneous equation (40) can be readily solved by assuming a solution of the form

$$w(z) = \sum_n a_n w_n \quad , \tag{48}$$

which can be substituted into the equation to be solved yielding

$$\sum_n (\ell a_n w_n + \lambda^2 z a_n w_n) = c_o z^{p+1} V(z) \quad . \tag{49}$$

Using equation (42) we simplify the above equation by writing

$$\sum_n (\lambda^2 - \lambda_n^2) a_n w_n = \frac{c_o z^{p+1} V(z)}{z} \quad . \tag{50}$$

Next we express the right-hand side of the above equation as a series of orthogonal functions, that is,

$$\sum_n A_n w_n = \frac{c_o z^{p+1} V(z)}{z} \quad . \tag{51}$$

We evaluate the coefficients by multiplying both sides of equation (51) by w_m and integrating over the interval, that is,

$$\sum_n \int_0^{a^{1/2}} dz z A_n w_n w_m = c_o \int_0^{a^{1/2}} dz z^{p+1} V(z) w_m \quad . \tag{52}$$

Because of the orthogonality relation of equation (43) we may write

$$A_n \int_0^{a^{1/2}} dz z w_n^2 = c_o \int_0^{a^{1/2}} dz z^{p+1} V(z) w_n \quad , \tag{53}$$

where the integral of the left-hand side has been evaluated[10] as

$$\int_0^{a^{1/2}} dz z [J_p(\lambda_n z)]^2 = a/2 [J_{p+1}(\lambda_n a^{1/2})]^2 \quad . \tag{54}$$

Substitution of equation (51) into (50) and equation (54) into (53) yields

$$a_n = \frac{A_n}{\lambda^2 - \lambda_n^2} = \frac{\int_0^{a^{1/2}} dz z z^p V(z) J_p(\lambda_n z)}{\frac{a}{2} J_{p+1}^2 (\lambda_n a^{1/2})(\lambda^2 - \lambda_n^2)} \quad . \tag{55}$$

Finally, after combining equations (55), (48), and (54) we write that

$$S(z) = \sum_n \frac{2/a}{J_{p+1}^2(\lambda_n a^{1/2})} \int_0^{a^{1/2}} \mu\mu^p V(\mu) J_p(\lambda_n \mu) d\mu \, \frac{z^{-p} J_p(\lambda_n z)}{\lambda^2 - \lambda_n^2} \quad , \quad (56)$$

where we note that the integral is the Fourier-Bessel Series of $z^p V(z)$ and $z^{-p}J_p(\lambda_n z)$ are the normal modes. This equation can be written more compactly as

$$S(z) = \frac{2}{a} \sum_n \int_0^1 \frac{\mu^{p+1} V(\mu) J_p(\lambda_n \mu) J_p(\lambda_n z)}{J_{p+1}^2(\lambda_n a^{1/2}) z^p (\lambda^2 - \lambda_n^2)} \, d\mu \quad , \quad (57)$$

where the problem's Green's function or impulsive response is

$$G(z,\mu) = \sum_n \frac{(\mu/z)^p \mu J_p(\lambda_n \mu) J_p(\lambda_n z)}{\frac{a}{2} J_{p+1}^2(\lambda_n a^{1/2})(\lambda^2 - \lambda_n^2)} \quad . \quad (58)$$

Plots of the normal modes, $z^{-p}J_p(\lambda nz)$, normalized to unity at $\xi = 1$ are shown versus cylinder position in figure 3. Elements of the approximate solution of equations (21) and (36) are evident in the plot. The lower-order modes show the approximately linear growth of equation (21) and the higher-order modes show the inverse tension (i.e., $(1 - \xi)^{-1}$) behavior of equation (36). As expected, the complete solution integrates the two physical characteristics that are highlighted in the approximate solutions, that is, (1) the cylinder attempts to align with the flow leading to a linear growth in the transverse displacement, but (2) the cylinder is impeded by cylinder tension stiffness that increases as one moves forward along the cylinder and increases with wavenumber increase. The frequency or wavenumber dependence will be determined by the magnitude of the various modes which, in turn, are obtained from the Fourier-Bessel spectrum of $z^pV(z)$. Unfortunately, the spectrum of a planewave is rather broad, so the series of equation (56) does not rapidly converge. In fact, equation (56) is not a numerically efficient approach to obtaining solutions. A method for generating numerical solutions is discussed in the next section.

The wavenumber, or equivalently frequency, dependence of the system is analytically determined by the wavenumber dependence of the Fourier-Bessel spectra discussed above and the frequency dependence of the $(\lambda^2 - \lambda_n^2)^{-1}$ term in equation (56). Using the parameters defined in equation (38) we write

$$\lambda^2 - \lambda_n^2 = b_o^2 - \delta_n^2/a \quad ,$$

where δ_n is the n^{th} real zeros of the p^{th} order Bessel function. Employing the assumptions discussed following equations (45) and (47) and the parameters defined in equation (38) we write

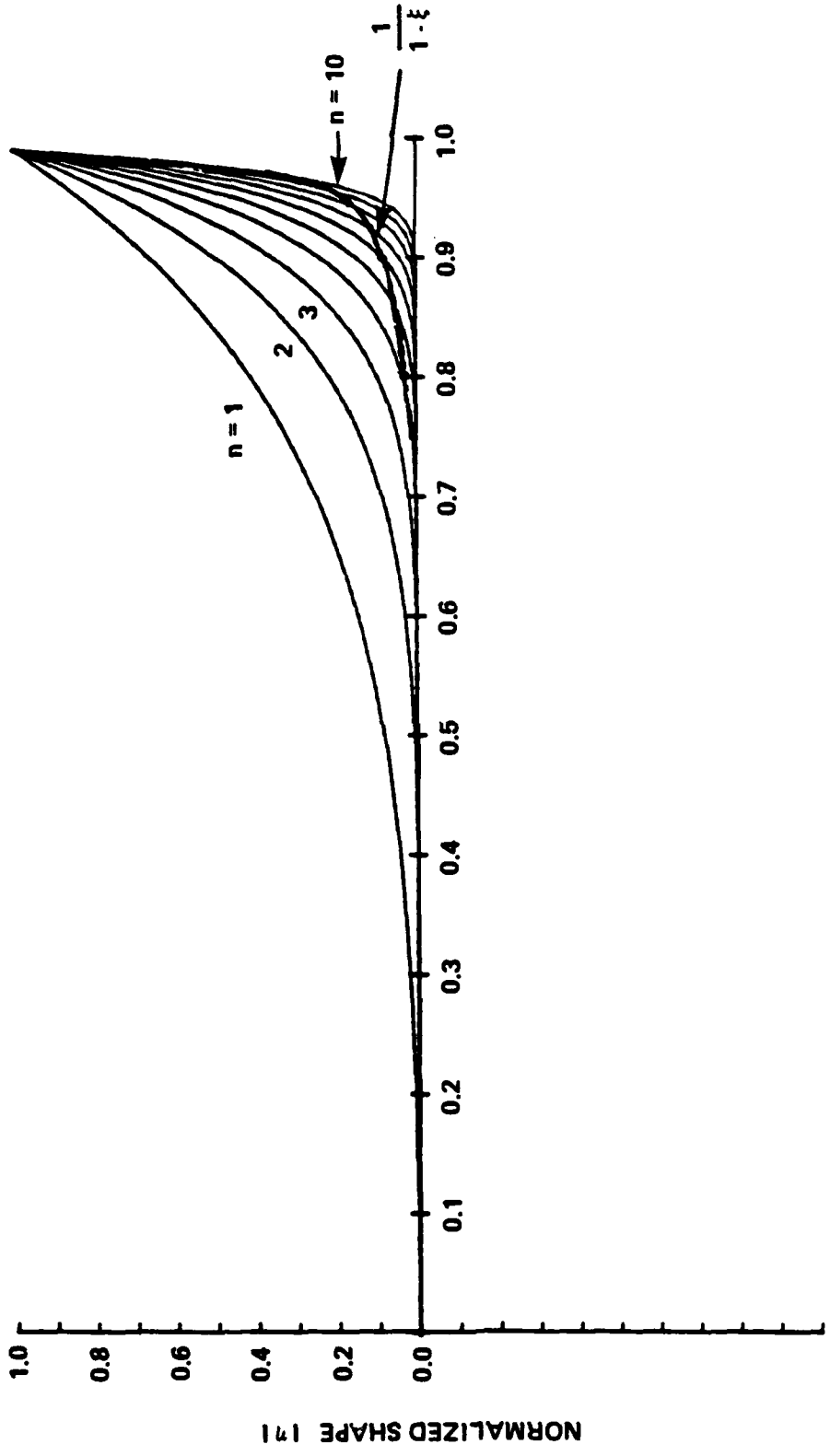

Figure 3. Modal Shapes

$$\lambda^2 - \lambda_n^2 \cong -i4 \frac{c_n}{\pi c_t} \omega + \frac{\delta_n^2}{2\beta c_t \varepsilon}$$

$$\lambda^2 - \lambda_n^2 \cong -\frac{4c_n}{\pi c_t} \left(i\omega + \frac{\pi \delta_n^2}{8\beta c_n \varepsilon} \right) .$$

Therefore, we conclude that $(\lambda^2 - \lambda_n^2)^{-1}$ is a simple pole reflecting viscous damping of transverse motion. In other words, the "velocity" or "dashpot" damping of equation (5) leads to a $(i\omega)^{-1}$ dependence.

5. NUMERICAL SOLUTIONS

The analytical solution of section 4 has given a better physical understanding of the process by identifying the constitute modes of behavior of the system. The method is not, however, a numerically efficient way of realizing specific space-time array shapes. In this section an efficient method of obtaining a numerical solution is described.

A solution to the forced vibration problem of equation (7b) using a finite difference scheme in conjunction with powerful numerical ordinary differential equation methods is described in reference 8. The method of reference 8 has been expanded to solve the current problem of interest summarized in equation (7c).

Reference 8 details the procedures which are merely summarized here for reader convenience.

We proceed by applying the second-order central and backward discre ization to the partial differential equation (7) in the ξ direction. This yields the form

$$\frac{\partial^2 \eta_m}{\partial \tau^2} + (a + b\xi_m) \left(\frac{\eta_{m+1} - 2\eta_m + \eta_{m-1}}{h^2} \right) + \frac{c}{h} (\eta_m - \eta_{m-1}) + \frac{2\beta}{h} \frac{\partial}{\partial \tau} \left(\eta_m - \eta_{m-1} \right) + d \frac{\partial \eta_m}{\partial \tau} = -dV_m \tag{59}$$

where

$$\xi_m = mh, \eta_m = \eta(\xi_m, \tau), \text{ and } V_m = V(\xi_m, \tau) \quad .$$

Equation (59) is a difference equation representing a system of second-order ordinary differential equation and is an approximation of equation (7). This is converted to a system of first-order ordinary differential equations by substitution of

$$\frac{d\eta_1}{d\tau} = w_1 \quad \text{and} \quad \frac{d\eta_2}{d\tau} = w_2 \tag{60}$$

into equation (59). After some manipulation the first-order system may be written in matrix form as

$$\frac{d}{d\tau} N = A(\xi)N + g(\xi,\tau,\eta) \qquad (61)$$

where

$$N = \begin{bmatrix} \eta_1 \\ w_1 \\ \eta_2 \\ w_2 \\ \cdot \\ \cdot \\ \cdot \\ \eta_{M-1} \\ w_{M-1} \end{bmatrix} \quad \text{and} \quad g = \begin{bmatrix} 0 \\ \frac{2\beta}{h} w_o + \frac{c}{h} \eta_o - dV_1 \\ 0 \\ -dV_2 \\ \cdot \\ \cdot \\ \cdot \\ 0 \\ -\frac{a + b\xi_{M-1}}{h^2} \eta_M - dV_{M-1} \end{bmatrix}$$

and M is the number of spatial points.

The g vector contains only the boundary conditions and nonhomogeneous forcing particular to the present problem. The $A(\xi)$ matrix contains no forcing terms at all and thus represents a known linear transformation. The difference between the above equation and equation (3.10) of reference 8 is the inclusion of the nonhomogeneous terms. These terms are inputs to the problem in the same sense as boundary conditions are inputs. Thus, the solution of equation set (61) can proceed exactly as it did in reference 8 using the generalized Adams-Bashforth method — a highly efficient procedure for this type of problem.

Application of the upstream (or top) boundary condition of equation (7c) makes $w_o = \eta_o = 0$ in the g vector. However the boundedness condition of equation (7c) does not adequately specify η_M which is an explicit value of the downstream (or bottom) boundary condition. This is an important difficulty associated with the application of these techniques to this particular problem (refer to the discussion of boundary conditions in section 2 of this report). However, because the existence of the nonhomogeneous term in the present problem in no way modifies the downstream boundary condition, we may use the approximate ad hoc condition derived in reference 8. The approach was to integrate the transverse momentum equation (equation (1)) over a short tapered end which is attached to the free end in order to generate the required boundary condition. The result of this approach is the condition

$$\frac{\partial \eta}{\partial \xi} + \frac{\partial \eta}{\partial \tau} = 0 \quad , \qquad (62)$$

which is shown in reference 8 to adequately solve the problem. Physically this condition represents a "radiation condition" which reflects no energy.

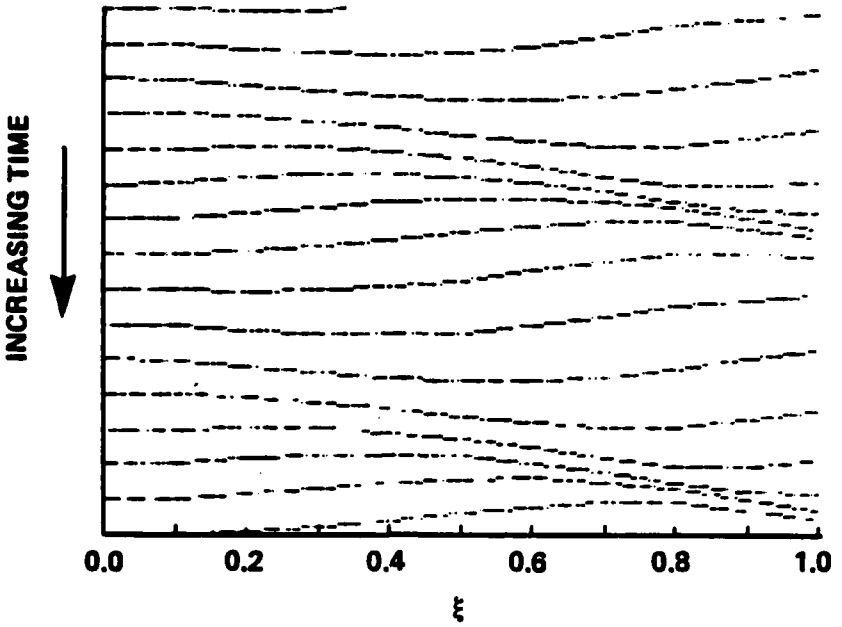

Figure 4a. Spatial Cylinder Shapes

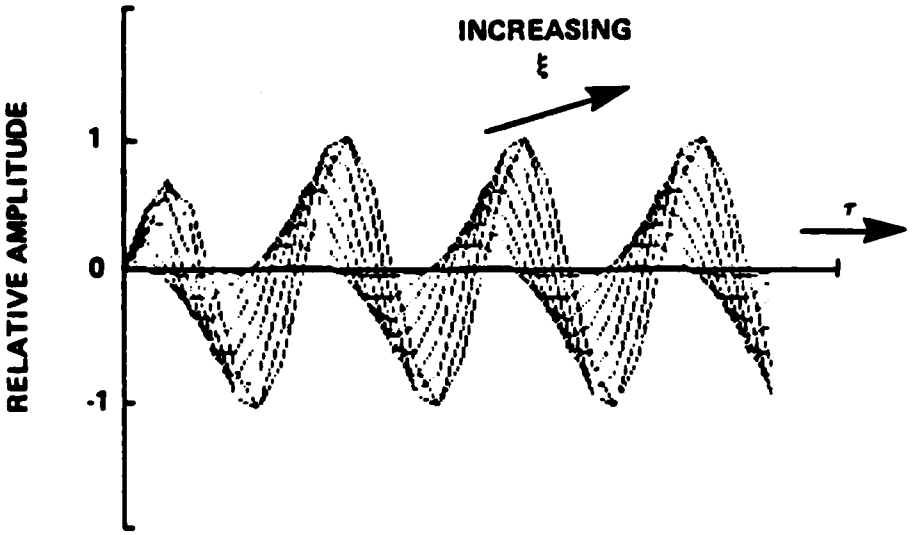

Figure 4b. Temporal Cylinder Shapes

Figure 4. Cylinder Shapes

As was the case in the previous two sections, we are interested in solutions to the "planewave" case discussed in section 2. This was accomplished by numerically solving an initial value problem having the following conditions

$$\eta(\xi,0) = 0 \quad \text{for } 0 \le \xi \le 1,$$

$$\frac{d\eta(\xi,0)}{d\tau} = 0 \quad \text{for } 0 \le \xi \le 1, \text{ and} \tag{63}$$

$$V(\xi,\tau) = e^{i(\omega\tau - k\xi)} \quad \text{for } 0 \le \xi \le 1 \quad .$$

The results of the technique are displayed in two ways: (1) transverse displacement (η) versus longitudinal position (ξ) with time (τ) as a parameter, and (2) transverse displacement versus time with longitudinal position as a parameter. In the first type of display (figure 4a), each sequential time increment is offset downward in a "waterfall" type display. These displays show qualitatively the two characteristics of the solution discussed in the previous two sections, that is, (1) the solution appears to propagate aft with unity nondimensional phase velocity which in dimensional quantities is the axial flow velocity, U; and (2) the envelope of the solutions grows in the downstream direction. The latter phenomenon is better illustrated in figure 4b which shows that the time periodic steady state response increases downstream, that is, increasing ξ.

6. SUMMARY

It has been shown that the transverse dynamics of a long flexible cylinder immersed in axial fluid flow and perturbed by a space-time nonaxial flow component can be modeled by a linear nonhomogeneous PDE. The subject momentum equation is related to a previously studied forced vibration problem that was modeled by a similar homogeneous PDE. The intent of this work is to model the transverse dynamics of a cable/array system driven by crosscurrents, and to relate it to a previous study of a cable/array system excited by the random crosstrack meandering of the towing vessel.

Three types of analytical solutions were explored in order to develop a physical and mathematical understanding of the ocean-induced transverse motion of towed arrays. The following physical picture emerges from this effort:

1. In cable/array systems having aspect ratios (length to diameter) greater than 10^5, inertial forces can be neglected.

2. If the cable/array system length is much shorter than the alongtrack wavelength of the oceanic current system, then hydrodynamic forces dominate structural forces and the cable/array locally aligns with the flow. Transverse displacements are then the spatial integral of the cable/array angle with the fluid. The displacement response of the system will be proportional to $\hat{V}/Uk$, and these displacements will appear to propagate aft at nearly the tow speed.

3. If the cable/array system length is much longer than the alongtrack wavelength of the oceanic current system, then the tension stiffness of the cylinder is the principal impedance to the transverse ocean forces applied to the cable. The consequence of this fact is that the attenuation of the transverse dynamics by tension stiffness is very much a function of the spatial position on the cylinder and the alongtrack wavenumber of the ocean current. Because the tension goes to zero at the free end, the dynamics near the free end are larger relative to upstream positions. Displacement response of the system will be proportional to $(\hat{V}/U)(c_n/\pi c_t)/k^2(L - x)$, where $c_n/\pi c_t$ is a measure of the normal to transverse hydrodynamic drag. These displacements will appear to propagate aft at nearly the tow speed and grow significantly near the free end.

4. Normal hydrodynamic drag acts as a "velocity" or "dashpot" damper yielding a frequency-dependent dissipation term proportional to $(\omega)^{-1}$.

5. The magnitude of the "tail" dynamics relative to upstream positions is a function of wavenumber, or equivalently apparent frequency, of the oceanic current process. At small wavenumbers, where hydrodynamic forces dominate structural stiffness, little "tail wagging" will be observed. At large wavenumbers the envelope of the "tail wagging" will be proportional to $(L - x)^{-1}$.

6. The actual response of a cable/array system to ocean-forcing is determined by the Fourier-Bessel spectra of a function of the spatial distribution of the crosstrack ocean-current structure. Such spectra need to be studied to determine the actual spectra of ocean-induced cable/towed array transverse dynamics.

7. The transverse shape of a cable/array system can be generally expressed as a sum of "modes" of the form $z\text{-}pJ_p(\lambda nz)$. The convergence of this sum, for the case of planewaves and impulsive spatial structures, is rather slow, so this procedure is not a very numerically efficient method of solution.

8. A numerical solution to the subject governing equation which uses a finite difference scheme (i.e., "method of lines") in conjunction with powerful numerical ordinary differential equation methods (i.e., "generalized Adams-Bashforth" method) has been programmed and examples run.

There are three general areas of future work necessary to understand the ocean-induced towed array dynamics problem: (1) further quantitative comparison between analytical and numerical procedures is necessary to give credibility to the numerical technique; (2) the Fourier-Bessel spectra of typical high wavenumber ocean processes, such as internal waves and upper ocean turbulence, are needed to understand what structural modes will be excited; and (3) a quantitative comparison between theory and existing data is needed to give credibility to this modeling procedure.

REFERENCES

1. R. M. Kennedy and E. S. Strahan, "A Linear Theory of Transverse Cable Dynamics at Low Frequencies," NUSC Technical Report 6463, Naval Underwater Systems Center, New London, CT, 5 June 1981.

2. R. M. Kennedy, "Low-Frequency Motion Response of Cable Towed Array Systems," NUSC Technical Memorandum No. 93231, Naval Underwater Systems Center, New London, CT, July 1979.

3. R. M. Kennedy and F. A. Galletta, "Cable Dynamics Experiment Final Report," NUSC Technical Report 6467, Naval Underwater Systems Center, New London, CT, October 1981.

4. M. P. Paidoussis, "Dynamics of Flexible Slender Cylinders in Axial Flow," *Journal of Fluid Mechanics*, vol. 26, 1966, pp. 717-751.

5. C. R. Ortloff and J. Ives, "On the Dynamic Motion of a Thin Flexible Cylinder in a Viscous Stream," *Journal of Fluid Mechanics*, vol. 38, part 4, 1969, pp. 713-720.

6. P. P. Rispin, "Normal Drag on Thin Flexible Cylinders at Shallow Angles," to be published.

7. M. J. Lighthill, "Note on the Swimming of Slender Fish," *Journal of Fluid Mechanics*, vol. 9, 1960, p. 305.

8. D. Lee and R. M. Kennedy, "A Numerical Treatment of the Dynamic Motion of a Zero Bending Rigidity Cylinder in a Viscous Stream," NUSC Technical Report 6343, Naval Underwater Systems Center, New London, CT, February 1981.

9. R. M. Kennedy, H. P. Bakewell, and W. C. Zimmerman, "Normal and Tangential Hydrodynamic Drag of Very Thin Cylinders in Near Axial Flow," NUSC Technical Report 6811, Naval Underwater Systems Center, New London, CT, February 1983.

10. F. B. Hildebrand, *Advanced Calculus for Engineers*, Prentice-Hall, Inc., Englewood Cliffs, NJ, pp. 18-19.

11. J. Ketchman, "Vibration Induced in Towed Linear Underwater Array Cables," *IEEE Journal of Oceanic Engineering*, vol. OE-6, no. 3, July 1981.

INITIAL DISTRIBUTION LIST

Addressee	No. of Copies
APL, University of Washington, Dr. D. E. Calkins	1
Bendix Corp., Dr. F. DeMetz	1
BBN, Dr. S. Africk, D. Wagner	2
C&K Associates, C. Campbell	1
Chase Inc., Dr. D. Chase	1
Dunn & Associates, Dr. S. Dunn	1
DTNSRDC, Dr. P. P. Rispin	1
EG&G/WASC, F. Galletta	1
G&R Associates, S. Gardner	1
Hydrotronics, Inc.; G. Desmarais, Fort Lauderdale; Dr. S. Berlin, Anaheim, California	2
Mar, Inc., Dr. L. King	1
NAVSEA (Code 63R, D. Porter, C. Smith, C. Walker) (Code PMS-409, CAPT D. Bulka)	4
NOSC, Dr. M. Shensa	1
NRL, Dr. A. Markowitz	1
TASC, Dr. J. D'Appolito	1
Technology Service Corp., Dr. L. Brooks	1
University of Connecticut, Dr. M. Wachman	1


NAVAL UNDERWATER SYSTEMS CENTER
USC

END

FILMED

3 -86

DTIC